

Reactivity of biological and synthetic hydroxyapatite towards Zn(II) ion, solid-liquid investigations

GIGLIOLA LUSVARDI, LEDI MENABUE*, MONICA SALADINI
 Dipartimento di Chimica, Università degli Studi di Modena e Reggio Emilia,
 Via G. Campi 183, 41100 Modena, Italy
 E-mail: menabue@unimo.it

The reaction of biological and synthetic hydroxyapatite $\text{Ca}_5(\text{PO}_4)_3\text{OH}$ (HAP) with Zn^{2+} ions is investigated as a function of $\text{Zn}^{2+}/\text{Ca}^{2+}$ molar ratio, time, temperature and electrolyte type (NaCl, NaHCO_3 , Na_2HPO_4) by means of pH, pZn, pCa measurements, in aqueous solution. Biological powdered HAP invariably affords an almost quantitative reaction, while Zn^{2+} precipitated only partially by reaction with cubelets of biological HAP. Using powdered biological HAP and synthetic HAP (dried at 100°C), the reaction with Zn^{2+} ion is fast and takes place without addition of precipitating anion; synthetic HAP (dried at 1000°C) reacts if free phosphate ions are present.

The solid phases separated after different reaction times are investigated by means of X-ray diffraction (XRD), IR, SEM techniques and elemental analysis (C,H,N). The solid phases contain $\text{Zn}_3(\text{PO}_4)_2 \cdot 4\text{H}_2\text{O}$ (Hopeite) at the beginning of reaction and $\text{CaZn}_2(\text{PO}_4)_2 \cdot 2\text{H}_2\text{O}$ (Scholzite) at the equilibrium.

© 2002 Kluwer Academic Publishers

1. Introduction

The formation of different types of phosphate minerals in synthetic and biological systems is affected by many factors, such as pH, temperature and composition of the system [1]. The compositional factor has a more significant effect than pH; of the calcium phosphates, the thermodynamically most stable form, under physiological conditions, is hydroxyapatite $\text{Ca}_5(\text{PO}_4)_3\text{OH}$ [2] (HAP), the main inorganic phase in the bones and teeth of vertebrates.

A peculiar feature of biologic HAP due to its small crystal size and high surface area, is its ability to accommodate many cationic or anionic impurities that can be adsorbed on the surface or give rise to ionic exchange [3]. The physico-chemical properties, such as lattice parameters, crystallinity, thermal and chemical stability of impure HAP, are influenced by the chemical nature of impurities. Adsorption of foreign ions generally does not affect the apatite structure, but substituents like F^- or CO_3^{2-} have readily detectable effects.

Among the metal ions present in biological apatites as trace elements, there is also Zn^{2+} [1]. Zinc, in particular, is essential for the development and growth of all species, including humans, and has been implicated with mineralization in biological systems. Zinc is found in all human tissues, with bone containing the major part of total body zinc [4]; the total body content of zinc amounts to $3 \cdot 10^4 \mu\text{mol}$, most of which is found in bone

and muscle. The important role of zinc in many biological functions, is well known: Zn is a cofactor for many enzymes and is essential for DNA replication. One of its applications is in dentistry in the form of zinc phosphate cement, which has been the cement of choice since 1879 [5,6]. It is a mixture of calcined powder ($1000\text{--}1200^\circ\text{C}$) and an aqueous solution: the basic constituent of the powder is ZnO (75–99%), while the principal modifier is MgO (7–13%) [7]. In addition, the powder may contain small amounts of other oxides such as bismuth and silicon oxides. The liquids are essentially phosphoric acid, water, Aluminum phosphate and, in some cases, zinc phosphate. When the powder is mixed with the liquid it sets, but the exact mechanism is not known. However, the setting reaction and resultant structure have been attributed to the formation of $\text{ZnHPO}_4 \cdot 3\text{H}_2\text{O}$ or $\text{Zn}_3(\text{PO}_4)_2 \cdot 4\text{H}_2\text{O}$ (Hopeite), a reaction that has been considered incomplete. Thus, the set cement consists of a distribution of the zinc and magnesium oxide particles cemented together with phosphates. In some cases the cement seems to release H^+ into the dental pulp giving rise to some problems [5] (as pulpal necrosis), but its role in dentine remineralization is clinically beneficial.

Previously [8] we carried out a study on the reaction between synthetic hydroxyapatite, of high crystallinity and low surface area, and Zn^{2+} ions by means of pH and ion measurements as a function of the time, temperature

*Author to whom correspondence should be addressed.

and salt composition, in the 1–0.1 Zn^{2+}/Ca^{2+} molar ratio. The results indicated that the Zn^{2+} ion does not form the species $ZnOH^+$ and the pH of the system Zn^{2+}/HAP was invariably greater than 6 (even upon addition of NaCl to give a total ionic strength of 0.15 mol dm^{-3}) and too high to promote HAP dissolution and subsequent reaction with Zn^{2+} . By lowering the pH to below 5, partial solubilization of HAP took place, accompanied by precipitation of $Zn_3(PO_4)_2 \cdot 2H_2O$ (JCDPS file no. 10-333) [9], but the Zn^{2+} ion was unable to replace the Ca^{2+} ion in the HAP structure, as was previously observed with the Cu^{2+} ion [10]. The addition of HCO_3^- ions (0.03 mol dm^{-3}) or of a mixture of HCO_3^- and HPO_4^{2-} , with a large excess of the former, brings about the formation of a poor soluble species such as $ZnCO_3$ (Smithsonite, JCDPS file no. 8-449) [9] which is the most stable phase in these experimental conditions, i.e. $pH > 6$ and very low phosphate concentration [11].

Here, using different types of HAP and focusing our attention on biological HAP, we investigate the HAP- Zn^{2+} system at different Zn^{2+}/Ca^{2+} molar ratios, pHs and in the presence of anions which form zinc (II) insoluble compounds (such as HCO_3^- and HPO_4^{2-}) and which are found in blood plasma [12], in order to evaluate the relative effects of HAP type and anions on the precipitation of Zn^{2+} ion and the solid phases formed.

2. Experimental

2.1. Starting materials

$ZnCl_2$ of analytical grade was from RIEDEL-DE HAEN, NaCl and $NaHCO_3$ of RPE-ACS grade were from C.ERBA, Na_2HPO_4 was from ALDRICH and were used as received; HAP synthetic (ALDRICH) was maintained at 1000°C for 1 h (hereafter HAP1) or 100°C for 48 h (hereafter HAP2), before use. Biological HAP (femoral bovine bone) was powdered

after mechanical removal of the surrounding connective tissue, washed in double-distilled water and maintained at 100°C for 48 h before use (elemental analysis for C, H, N was 7.34, 1.49, 1.87% respectively). We also used biological HAP of 2–3 mm of dimension, cubelets-like, prepared by means of mechanical cutting and treated as the powdered biological HAP. The ICP standards were prepared by diluting C.ERBA NORMEX solution. HNO_3 , for the preparations of ICP standards and samples, was from MERCK.

2.2. Preparation of the samples

The samples were prepared in double-distilled water from a concentrated aqueous solution of $ZnCl_2$ ($[Zn^{2+}] \cong 0.1 \text{ mol dm}^{-3}$) and standardized with ICP. The samples were prepared by adding, in a closed polyethylene flask, the appropriate volume of $ZnCl_2$ solution and double-distilled water to a total volume of 100 or 50 cm^3 (if using biological HAP) in order to obtain $[Zn^{2+}] = 10^{-2}$ or $2 \cdot 10^{-2} \text{ mol dm}^{-3}$ and the Zn^{2+} concentration was checked by ICP measurements. The solutions were thermostatted at 37°C for 30 min. and 1 gr or 0.5 gr (if biological) of HAP was added, which gave a Zn^{2+}/Ca^{2+} ratio in the range 0.1–0.2.

The ionic strength was adjusted to 0.15 mol dm^{-3} by the addition of electrolytes (NaCl for samples Ia and Ib, NaCl- Na_2HPO_4 for samples I, IV–VI and NaCl- $Na_2HPO_4 - NaHCO_3$ for samples III, VII).

Table 1 summarizes the sample numbers vs salt composition of the medium.

The concentration of M^{n+} in the starting solution was tested with ICP measurements, the samples were thermostatted at 37 and 60°C under continuous stirring and at different reaction times, the flasks were cooled at room temperature and, after allowing the sample solution to become clear, the supernatant liquid was withdrawn for ICP measurements. For each sample two withdrawals

TABLE I Summary of the sample type vs salt composition of the medium ($I = 0.15 \text{ mol dm}^{-3}$ $T = 37^\circ\text{C}$)

System	[NaCl]/ mol dm^{-3}	[Na_2HPO_4]/ mol dm^{-3}	[$NaHCO_3$]/ mol dm^{-3}	Note
Molar ratio $Zn^{2+}/Ca^{2+} = 0.1$				
Ia	0.12	—	—	HAP2
Ib	0.12	—	—	Biological HAP
II	0.09	0.01	—	HAP1
IIa	0.09	0.01	—	HAP2
IIb	0.09	0.01	—	Biological HAP
IIc	0.09	0.01	—	HAP1, $T = 60^\circ\text{C}$
IId	0.09	0.01	—	HAP2, $T = 60^\circ\text{C}$
III	0.10	0.005	0.005	HAP1
Molar ratio $Zn^{2+}/Ca^{2+} = 0.15$				
IV	0.09	0.005	—	HAP1
IVc	0.09	0.005	—	HAP1, $T = 60^\circ\text{C}$
Molar ratio $Zn^{2+}/Ca^{2+} = 0.2$				
V	0.06	0.01	—	HAP1
Va	0.06	0.01	—	HAP2
Vb	0.06	0.01	—	Biological HAP
Vc	0.06	0.01	—	HAP1, $T = 60^\circ\text{C}$
Vd	0.06	0.01	—	HAP2, $T = 60^\circ\text{C}$
VI	0.075	0.005	—	HAP1, $T = 60^\circ\text{C}$
VII	0.07	0.005	0.005	HAP1
VIIa	0.07	0.005	0.005	HAP2
VIIb	0.07	0.005	0.005	Biological HAP
VIIc	0.07	0.005	0.005	Biological HAP (cubelets)

were carried out and the change in volume of the samples was taken into account in each ICP measurement. For all samples the concentration of the metals was measured until equilibrium was reached. ICP measurements were performed with a Spectroflame Modula spectrometer.

At different time intervals (0.5 h–30 days), the samples were filtered in order to investigate the solid phase. The solids were washed with double-distilled water and dried for 24 h on P_2O_5 under vacuum.

2.3. pH Measurements

The pH change for the different $[Zn^{2+}]$ concentration and temperature values was recorded continuously by means of an Orion 420A pH meter equipped with a printer model 900A and Orion electrode Model No. 91-03, with automatic temperature compensation; the calibration of the electrode against NBS buffers was performed at intervals of 12 h.

2.4. X-ray powder diffraction

XRD analyses were carried out on finely powdered samples with a Philips PW3710-based automated diffractometer, using Ni-filtered $Cu-K\alpha_1$ radiation ($\lambda = 1.54060 \text{ \AA}$) in the $5^\circ \leq 2\theta \leq 65^\circ$ range with a step size of 0.03° and a time step of 2.5 s.

2.5. Infrared spectra

The IR spectra in the solid state, in the spectral range $4000\text{--}400 \text{ cm}^{-1}$, were performed on KBr pellets as support with a Perkin Elmer FT-IR mod1600 spectrometer. The pellets were prepared with *ca.* 0.7, 1, or 1.5 mg of sample mixed carefully to 200 mg of KBr.

2.6. Analysis

Elemental analysis (C, H, N) was performed with a C.Erba model 1106 elemental analyzer.

2.7. Scanning electron microscopy (SEM) and energy dispersive spectroscopy (EDS)

The morphological analyses were performed with a Philips PSEM 500, equipped with an energy dispersive X-ray analyzer (EDS, XL 40); the samples were mounted on a stainless steel stub using double-stick tape and then coated with Au and Pd.

2.8. Surface area measurements

The surface area was measured by means of the Brunauer-Emmett-Teller (BET) technique, using a Micromeritics Gemini 2360 Instrument.

3. Results

The surface area of HAP1, HAP2 and biological HAP is 2.81, 57.8 and $21.3 \text{ m}^2 \text{ g}^{-1}$, respectively and the corresponding powder patterns reveal that the broadness of the peaks is related to the crystallinity of the sample

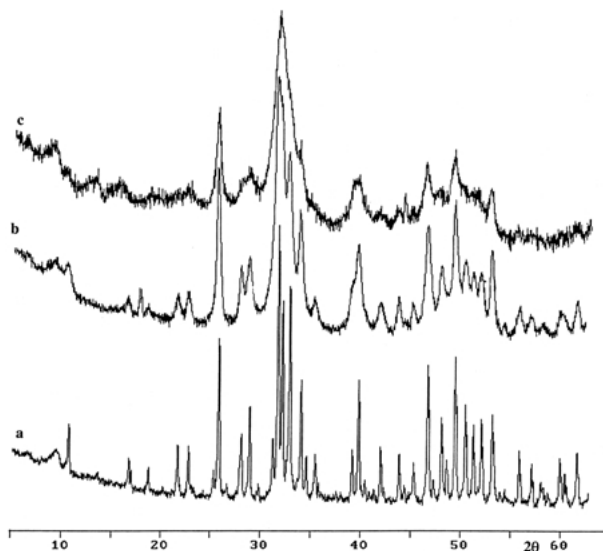


Figure 1 XRD powder spectra of: a, HAP1, b, HAP2 and c, biological HAP.

(Fig. 1). In the case of both synthetic HAP forms, the lines are more intense and less broad; their position and relative intensity correspond closely with the literature data (Hydroxyapatite, JCPDS file no. 9-432) [9]. The broadness of the peaks of HAP1 and HAP2 differs: peaks of HAP1 are the sharpest because of the heating of the sample.

We have also evaluated the Ca/P molar ratio for the different type of HAP by means of ICP plasma measurement and it is near the theoretical value of 1.67, 1.80 in all cases. The results obtained at different kinds of electrolytes are reported below.

3.1. NaCl

We prepared samples with $Zn^{2+}/Ca^{2+} = 0.1$ molar ratio, HAP2 (Ia), biological HAP (Ib) and the physiological ionic strength was obtained with NaCl.

The starting pH at 37°C , for samples Ia and Ib, is 4.60 and 5.80, respectively and in both cases increases during the reaction until the final, constant values of 5.65 and 7.25, respectively.

Biological HAP reacts promptly with Zn^{2+} ion: after 2 h the precipitation of Zn^{2+} ion is almost quantitative $pZn = 3.12$, (Fig. 2) ($[Zn^{2+}] = 7.5 \cdot 10^{-4} \text{ mol dm}^{-3}$) and can be considered complete after 15 days, $pZn = 4$, ($[Zn^{2+}] = 10^{-4} \text{ mol dm}^{-3}$). After 2 h, the Ca^{2+} concentration increases to the maximum, ($10^{-2} \text{ mol dm}^{-3}$), indicating a significant HAP dissolution despite the relatively high pH value ($\text{pH} \approx 5.85$); it subsequently decreases to $7 \cdot 10^{-3} \text{ mol dm}^{-3}$ after 15 d.

The XRD spectrum of the solid separated after 1 month of reaction is essentially unmodified with respect to that of HAP before reaction; a new weak line can also be observed in the $10\text{--}15^\circ 2\theta$ range, but because of its low intensity its assignment is difficult (Fig. 3a).

Using HAP2, the reaction is slow; after 2 h of contact the Zn^{2+} concentration is reduced by half and after 1 month $[Zn^{2+}] = 7 \cdot 10^{-4} \text{ mol dm}^{-3}$. The XRD spectrum of the solid separated after 2 h, show a new weak line as shoulder of the most intense line of HAP (31.75°), but because of its low resolution, we are not able to

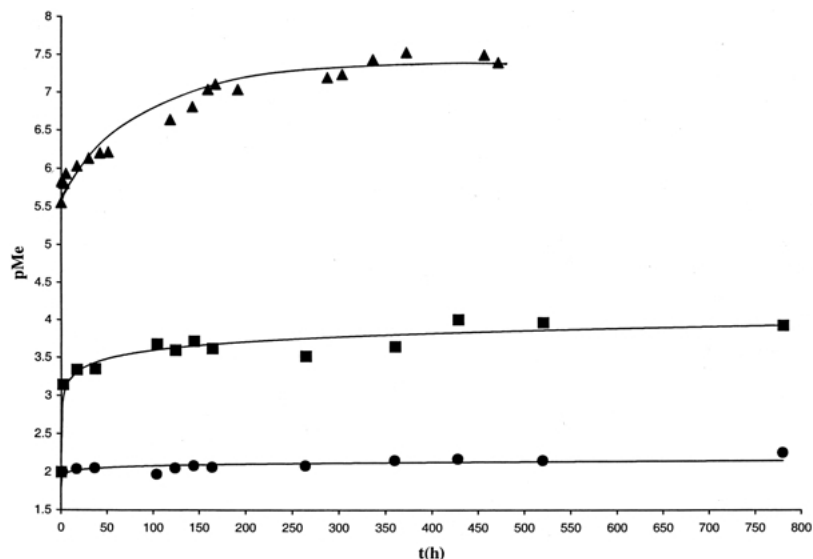


Figure 2 pH(▲), pZn(■) and pCa(●) vs. time for a molar ratio $Zn^{2+}/Ca^{2+} = 0.1$, biological HAP, $I = 0.15 \text{ mol dm}^{-3}$ adjusted with 0.12 mol dm^{-3} NaCl, $T = 37^\circ\text{C}$.

assign it; after 1 month (Fig. 3b), in addition to HAP we can identify $Zn_3(PO_4)_2 \cdot 4H_2O$ (Hopeite, JCPDS file no. 33-1474) [9] and the mixed compound $CaZn_2(PO_4)_2 \cdot 2H_2O$ (Scholizite, JCPDS file no. 29-1412) [9].

3.2. NaCl- Na_2HPO_4

We prepared samples at physiological ionic strength obtained with NaCl and Na_2HPO_4 , $Zn^{2+}/Ca^{2+} = 0.1$, (samples II–IId), 0.15 (sample IV), and 0.2 molar ratio (samples V–Vd) (Table 1). The systems are also studied at 60°C , (IIc, IId, Vc, Vd).

The starting pH at 37°C , for samples types II, IV, V are, respectively, 5.90 or 6.80 (synthetic or biological HAP), 4.15 and 4.00 or 5.00 (synthetic or biological HAP), depending on the Zn^{2+} and phosphate ion concentrations.

For all samples II–IId the concentration of phosphate

ion allows for the almost quantitative precipitation of Zn^{2+} over 30 min. ($[Zn^{2+}] \approx 10^{-4} \text{ mol dm}^{-3}$); at this time the Ca^{2+} concentration reaches the maximum ($1.5 \cdot 10^{-3} \text{ mol dm}^{-3}$).

The equilibrium is reached after 5 or 12 days, depending on HAP type: $[Ca^{2+}]$ decreases slowly to the constant value of $3 \cdot 10^{-4}$ (HAP1) or $10^{-3} \text{ mol dm}^{-3}$ (HAP2 and biological HAP). The final pH value is 5.50 for synthetic HAP and 6.50 for biological HAP.

The XRD powder spectra of the solids differ from one another depending on the reaction time. After 2 h, the spectrum is almost unchanged with respect to unreacted biological HAP (Fig. 4a,b); after 17 h of contact the spectrum (Fig. 4c) reveals, in addition to HAP, the presence of Hopeite as a minor crystalline phase; after 12 days of

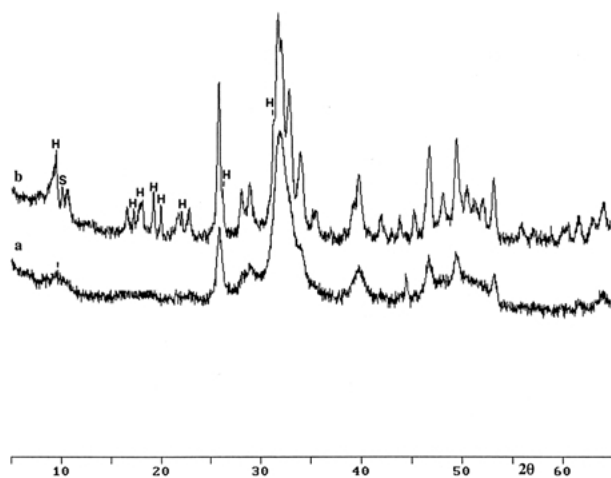


Figure 3 XRD powder spectra of the solids separated after 1 month of reaction with: a, biological HAP, b, HAP2; molar ratio $Zn^{2+}/Ca^{2+} = 0.1$, $I = 0.15 \text{ mol dm}^{-3}$ adjusted with 0.12 mol dm^{-3} NaCl, $T = 37^\circ\text{C}$. H = Hopeite ($Zn_3(PO_4)_2 \cdot 4H_2O$), S = Scholizite $CaZn_2(PO_4)_2 \cdot 2H_2O$.

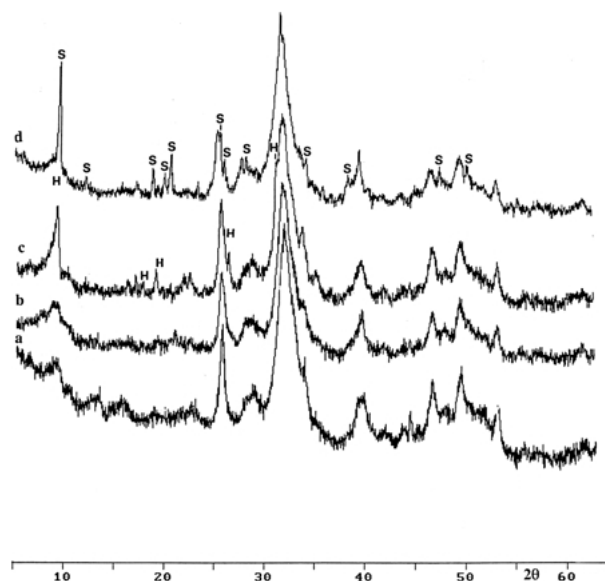


Figure 4 XRD powder spectra of a, biological HAP and of the solids separated from reaction with biological HAP, molar ratio $Zn^{2+}/Ca^{2+} = 0.1$, $I = 0.15 \text{ mol dm}^{-3}$ adjusted with 0.09 mol dm^{-3} NaCl and 0.01 mol dm^{-3} Na_2HPO_4 , $T = 37^\circ\text{C}$, after: b, 2 h; c, 17 h and d, 12 d of reaction. H = Hopeite ($Zn_3(PO_4)_2 \cdot 4H_2O$), S = Scholizite $CaZn_2(PO_4)_2 \cdot 2H_2O$.

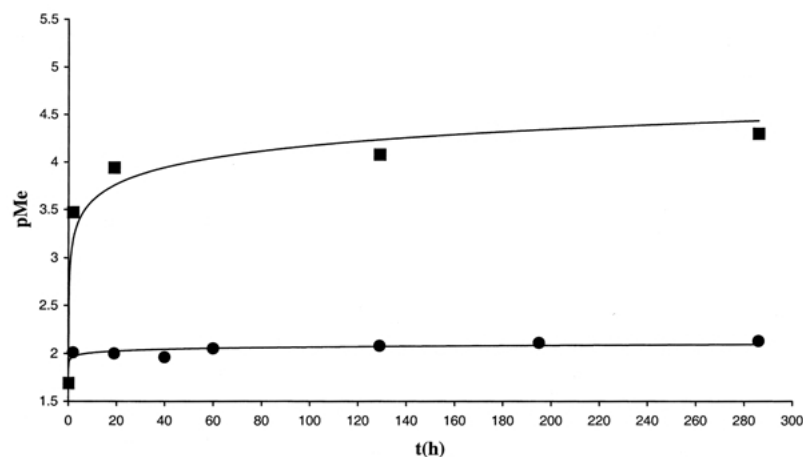


Figure 5 pZn(■) and pCa(●) vs. time for a molar ratio $Zn^{2+}/Ca^{2+} = 0.2$, biological HAP, $I = 0.15 \text{ mol dm}^{-3}$ adjusted with 0.06 mol dm^{-3} NaCl and 0.01 mol dm^{-3} Na_2HPO_4 , $T = 37^\circ\text{C}$.

reaction (Fig. 4d) the mixed phase Scholzite is present, in addition to HAP, with no evidence of the Hopeite lines. With HAP1, the behavior is similar but the new crystalline phase is already evident after 30 min. of contact.

In almost all cases, the lines of HAP are the most intense in the spectra; only in the spectra of HAP2, Scholzite lines predominate at the end of reaction.

When the phosphate ion fails, that means when its concentration is not sufficient to precipitate all Zn^{2+} , with respect to Zn^{2+} , using biological HAP (Vb) the reaction is fast and quantitative (Fig. 5): after 2 h $pZn \cong 3.50$ ($[Zn^{2+}] = 3.4 \cdot 10^{-4} \text{ mol dm}^{-3}$), and $pCa \cong 2.0$ ($[Ca^{2+}] = 9.7 \cdot 10^{-3} \text{ mol dm}^{-3}$), while pH increases to 5.12. After 12 days, with a pH of 5.20, pZn and pCa reach their respective equilibrium values of 4.30 and 2.10 ($[Zn^{2+}] = 5 \cdot 10^{-5}$ and $Ca^{2+} = 7.5 \cdot 10^{-3} \text{ mol dm}^{-3}$).

With both synthetic HAP, the reaction is slow and not quantitative. When pH decreases (Fig. 6), a fast and marked increase in pZn takes place, accompanied by decreases in pCa, due to HAP dissolution. In a few hours pH and pCa reach nearly constant values, while pZn gradually increases. Over 5–6 days pH and pZn reach their maximum values of 4.50 and 2.80, respectively ($[Zn^{2+}] \cong 1.6 \cdot 10^{-3} \text{ mol dm}^{-3}$), while $pCa \cong 2.10$

($[Ca^{2+}] = 8 \cdot 10^{-3} \text{ mol dm}^{-3}$). Afterwards, a reverse trend of pH and metal ion concentrations occurs until equilibrium is reached; after 25 days pH is 4.30, $pZn \cong 2.70$ and $pCa \cong 2.20$ ($[Zn^{2+}] = 2 \cdot 10^{-3}$ and $[Ca^{2+}] = 6 \cdot 10^{-3} \text{ mol dm}^{-3}$).

The XRD spectra of the solids separated after 2 h of contact (Fig. 7a), using biological HAP or HAP2, invariably reveal the presence of HAP and Hopeite: the lines of Hopeite are the most intense in the spectra. After 17 h and at the end of the reaction, the dominant lines are those of Scholzite (Fig. 7b, c) and in addition we could again identify HAP.

We also prepared samples with phosphate ions in further defect: the samples with $Zn^{2+}/Ca^{2+} = 0.15$ molar ratio were adjusted to $I = 0.15 \text{ mol dm}^{-3}$ with $[NaCl] = 0.09 \text{ mol dm}^{-3}$ and $[Na_2HPO_4] = 0.005 \text{ mol dm}^{-3}$ (IV) and the samples with $Zn^{2+}/Ca^{2+} = 0.2$ molar ratio were adjusted to $I = 0.15 \text{ mol dm}^{-3}$ with $[NaCl] = 0.075 \text{ mol dm}^{-3}$ and $[Na_2HPO_4] = 0.005 \text{ mol dm}^{-3}$ (VI); we also performed the study at 60°C (IVc).

In these cases the behavior of ion concentration resembles that of the type V samples, with a slight overall decrease in pH ($\Delta pH = -0.45$). The solid state confirms the results of previous systems.

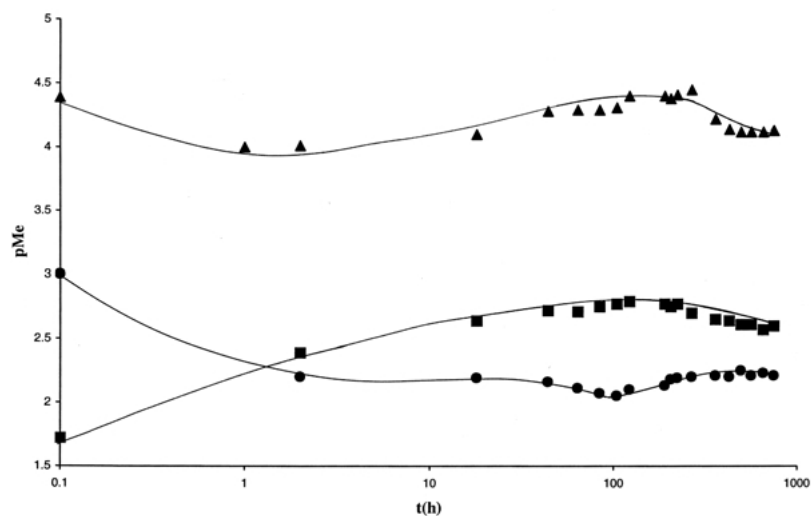


Figure 6 pH(▲), pZn(■) and pCa(●) vs. time for a molar ratio $Zn^{2+}/Ca^{2+} = 0.2$, HAP1, $I = 0.15 \text{ mol dm}^{-3}$ adjusted with 0.06 mol dm^{-3} NaCl and 0.01 mol dm^{-3} Na_2HPO_4 , $T = 37^\circ\text{C}$.

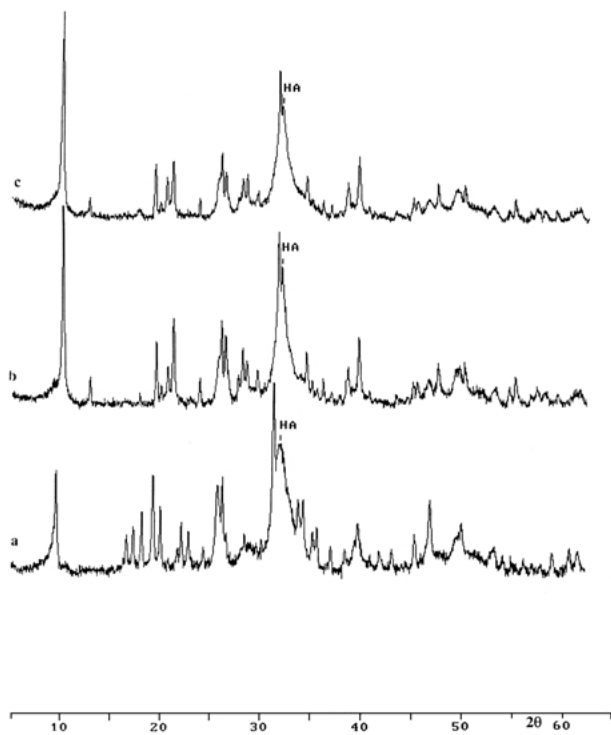


Figure 7 XRD powder spectra of solids separated from reaction with biological HAP, molar ratio $Zn^{2+}/Ca^{2+} = 0.2$, $I = 0.15 \text{ mol dm}^{-3}$ adjusted with 0.06 mol dm^{-3} NaCl and 0.01 mol dm^{-3} Na_2HPO_4 , $T = 37^\circ\text{C}$, after: a, 2h; b, 17h and c, 12d of reaction. HA = hydroxyapatite ($Ca_5(PO_4)_3 \cdot OH$).

3.3. $NaCl-Na_2HPO_4-NaHCO_3$

For sample III, $Zn^{2+}/Ca^{2+} = 0.1$ molar ratio (Table I) the precipitation of Zn^{2+} ion occurs immediately and quantitatively; the XRD technique on solid separated after 10 days reveals the lines of HAP, the main phase, Hopeite and new lines at low intensity probably belonging to those of $CaCO_3 \cdot 6H_2O$ (JCPDS File no.37-416) [9] (not showed).

Starting pH is in the range 4.80–5.50 for samples VIIa, VII–VIIb; with biological HAP the reaction is fast and quantitative: equilibrium is reached after 2 days. pH increases to 6.50, pZn and pCa are respectively 3.70 and 2.00, (Fig. 8) ($[Zn^{2+}] = 2 \cdot 10^{-4}$ and $[Ca^{2+}] = 10^{-2} \text{ mol dm}^{-3}$). With synthetic HAP, the reaction is

slow and not quantitative: equilibrium is reached after about 5–6 days and a significant amount of Zn^{2+} still remains in solution ($[Zn^{2+}] = 7 \cdot 10^{-4}$ and $7.5 \cdot 10^{-3} \text{ mol dm}^{-3}$ for HAP2 and HAP1, respectively), $[Ca^{2+}]$ is $2 \cdot 10^{-2}$ and $2.5 \cdot 10^{-3} \text{ mol dm}^{-3}$, respectively, for HAP2 and HAP1; for all samples pH increases with $\Delta pH \cong 1$.

The XRD spectra on solids separated after 17h of contact reveal the presence of HAP and Hopeite: with biological HAP the most intense lines of the two phases have the same relative intensity (Fig. 9a). The final solid separated with biological HAP shows lines of HAP, the main phase, and Scholzite (Fig. 9b); with synthetic HAP the spectra show HAP and in addition Hopeite. For HAP1 there is a weak line, whose position corresponds fairly closely to the main line of $CaCO_3 \cdot 6H_2O$ [9].

Elemental analysis for C of the solid separated after 2 h of reaction from synthetic HAP (initial C content for synthetic HAP is $\approx 0.18\%$) reveals a carbon content of 0.87% that gradually decreases to $\approx 0.21\%$ by the end of the reaction.

We also prepared sample VIIc by using 3 mm cubelets of biological HAP whose behavior reflects the reduction in reaction surface: the final Zn^{2+} and Ca^{2+} content are $2.5 \cdot 10^{-3}$ and $8.7 \cdot 10^{-3} \text{ mol dm}^{-3}$, respectively.

In this case, a morphological investigation by means of SEM and EDS was also carried out. The micrograph of Fig. 10 shows a variable distribution of the elements, which is related to the presence of a new matrix (Fig. 10a,b) in addition to the old matrix (Fig. 10c). The peak belonging to zinc (Fig. 11a), is more intense in the clear zone (Fig. 10a), the inverse trend for the peak belonging to calcium. This may well indicate the presence of a zinc-containing phase that is not uniformly distributed but localized. The same investigation was carried out on the solid separated after reaction of powdered biological and synthetic hydroxyapatite with zinc ion ($[Zn^{2+}] = 10^{-2} \text{ mol dm}^{-3}$); in this case, the ion distribution was homogeneous on the solid surface of the samples.

Infrared spectra (not showed) also confirm the presence of a Zn^{2+} -containing phase as revealed by means of XRD diffraction data. In fact, in the region between 550 and 650 cm^{-1} the intensity of the bands are

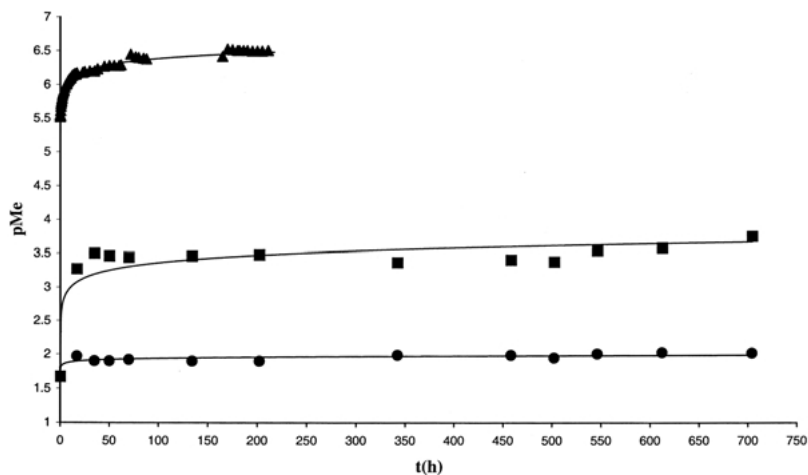


Figure 8 pH(\blacktriangle), pZn(\blacksquare) and pCa(\bullet) vs. time for a molar ratio $Zn^{2+}/Ca^{2+} = 0.2$, biological HAP, $I = 0.15 \text{ mol dm}^{-3}$ adjusted with 0.07 mol dm^{-3} NaCl, $0.005 \text{ mol dm}^{-3}$ Na_2HPO_4 and $0.005 \text{ mol dm}^{-3}$ $NaHCO_3$, $T = 37^\circ\text{C}$.

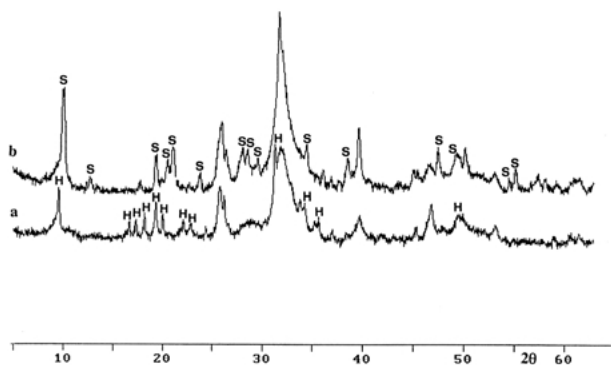


Figure 9 XRD powder spectra of solids separated from reaction with biological HAP, molar ratio $Zn^{2+}/Ca^{2+} = 0.2$, $I = 0.15 \text{ mol dm}^{-3}$ adjusted with 0.07 mol dm^{-3} NaCl, $0.005 \text{ mol dm}^{-3}$ Na_2HPO_4 , and $0.005 \text{ mol dm}^{-3}$ $NaHCO_3$ $T = 37^\circ\text{C}$, after: a, 17h and b, 1 month of reaction. H = Hopeite $Zn_3(PO_4)_2 \cdot 4H_2O$, S = Scholzite $CaZn_2(PO_4)_2 \cdot 2H_2O$.

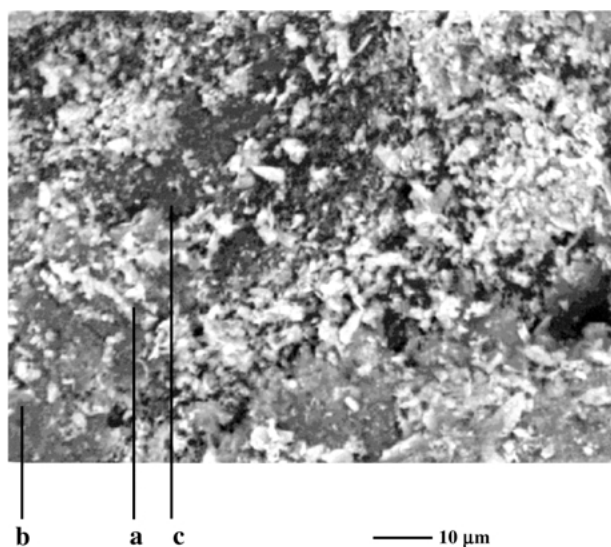


Figure 10 Scanning electron micrograph of biological HAP (cubelets) after 1 month of reaction molar ratio $Zn^{2+}/Ca^{2+} = 0.2$, $I = 0.15 \text{ mol dm}^{-3}$ adjusted with 0.06 mol dm^{-3} NaCl, $0.005 \text{ mol dm}^{-3}$ Na_2HPO_4 , and $0.005 \text{ mol dm}^{-3}$ $NaHCO_3$, $T = 37^\circ\text{C}$.

higher than to those of pure HAP and it is possible to identify an additional weak band at *ca.* 950 cm^{-1} . This could indicate the presence of Hopeite, in agreement with published data [13]. The behavior is similar for the different kinds of HAP; only in the case of biological HAP is the resolution of the spectra sometimes poor.

In our experimental conditions, the type of zinc-containing phase is in agreement with the field stability of zinc-compounds, in the presence of phosphate and carbonate ions [11].

In all the samples the concentration of Na^+ ion is unchanged at the end of reaction, and if we perform the reaction at 60°C , we observe a similar pattern.

4. Discussion

The high surface area of biological HAP and HAP2 exerts a fundamental influence on their behavior towards the Zn^{2+} ion; at physiological conditions of temperature and ionic strength, without precipitating anions, a fast reaction occurs, and in the case of biological HAP the

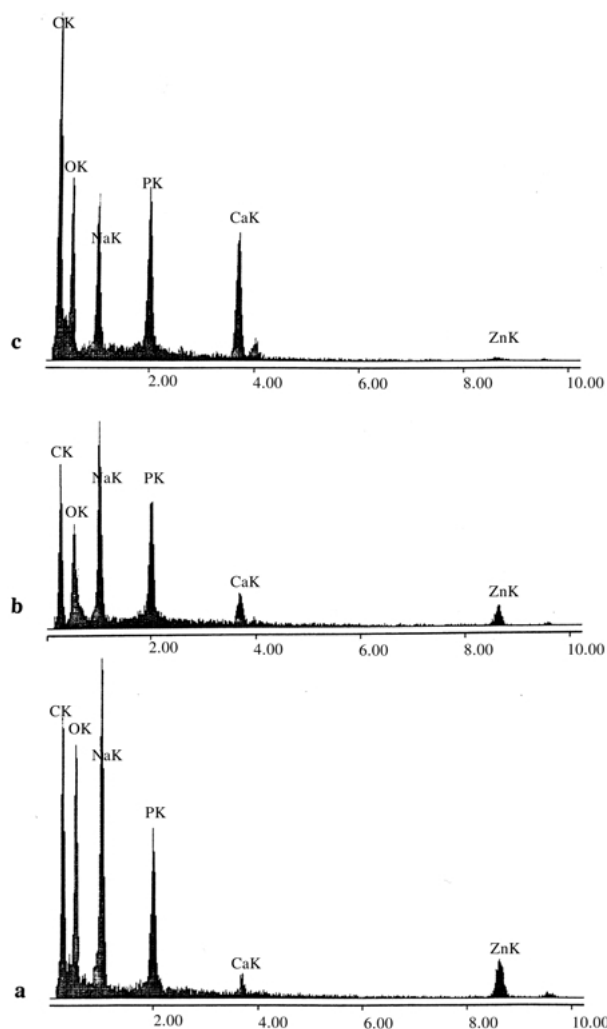
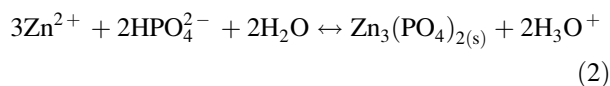


Figure 11 Energy dispersive spectra related to Fig. 10, of: a, new matrix (clear zone); b, new matrix; c, old matrix.

precipitation of the metal ion from the solution, is complete. The relatively high pH value does not inhibit the reaction. In these conditions we can hypothesize that, at the beginning of the reaction, the Zn^{2+} ion is removed by two processes: (a) adsorption on the HAP surface, made possible by the relatively high HAP surface and its low grade of crystallinity (Fig. 1c), according to the high rate of precipitation and the absence of a new crystalline phase during 15d; (b) HAP dissolution, according to the sharp increase in Ca^{2+} concentration, observed after 2 h of reaction. Previously we observed that HAP1, which presents a very low surface area and high crystallinity in the same experimental conditions, does not react with Zn^{2+} ion.

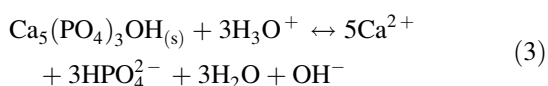
The presence of Zn^{2+} -precipitating anions such as phosphate, gives rise to a pattern related to phosphate concentration that is different from that of the Zn^{2+} ion.

At $[Zn^{2+}] = 0.01 \text{ mol dm}^{-3}$ and $[PO_4^{3-}] = 0.01 \text{ mol dm}^{-3}$, the process begins immediately with formation of Hopeite, with non-significant HAP dissolution; pH increases to near physiological levels and we can postulate the following reactions:



The salt formula and the pH observed, indicate that, at this stage, the reaction does not involve HAP because the phosphate ion exceeds that necessary for quantitative Zn^{2+} precipitation. In fact, assuming $[Zn^{2+}] = 0.01 \text{ mol dm}^{-3}$, the required stoichiometric concentration of HPO_4^{2-} is approximately $0.007 \text{ mol dm}^{-3}$, so the excess of phosphate buffers the H_3O^+ produced in Equation 2 and retards HAP dissolution, and in the XRD powder spectra the main phase is HAP. If Na_2HPO_4 is failing $[Zn^{2+}] = 0.02 \text{ mol dm}^{-3}$ and $[PO_4^{3-}] = 0.01 \text{ mol dm}^{-3}$, the behavior of biological HAP and HAP2 is similar to that observed in the absence of phosphate and we propose the same processes for Zn^{2+} removing.

In the case of HAP1, taking into account the experimental conditions of pH, we hypothesize reaction (3), in addition to reaction (2), in order to explain the trend of ion concentrations (Fig. 6):



Initially, in view of the high Zn^{2+} concentration, reaction (2) prevails, which corresponds to formation of Hopeite, and pH drops, so HAP dissolution takes place (reaction (3)), with the observed subsequent increase in pH and Ca^{2+} content. The increases in Ca^{2+} content favors the subsequent formation of Scholzite. This compound is probably formed mainly by the conversion of an amorphous zinc-containing phase due to adsorption of Zn^{2+} on the HAP surface and, to a lesser extent, to the conversion of crystalline phase, Hopeite, but also because of the slight difference in stability of Hopeite and Scholzite [11]. In fact, Scholzite is only slightly more stable than Hopeite, so at high Zn^{2+} concentration Zn^{2+} phases of formula $Zn_3(PO_4)_2$ (Hopeite or amorphous compound) are favored, while at high Ca^{2+} concentration the mixed phase is favored.

An equimolar addition of phosphate and carbonate facilitates the reaction of biological and synthetic HAP, regardless of surface area, even at low phosphate concentration; only with powdered biological HAP is the reaction complete. In view of the solid phases identified and of the Ca^{2+} concentration we would suggest that the processes involving Zn^{2+} are the same as those postulated when the phosphate is failing, while Ca^{2+} can also separate as carbonate.

5. Conclusions

Biological HAP reacts with Zn^{2+} ion, irrespective of the HAP dimensions (for example cubelets) and of the pH value. Powdered biological HAP gives rise to almost quantitative precipitation of Zn^{2+} in a few hours, without

addition of phosphate ions to the system. The addition of phosphate ions also makes for a fast and quantitative reaction with formation of a mixed Zn/Ca phosphate as final phase. A new crystalline phase is already apparent after 2 h; at equilibrium the pH is weakly acidic and in the range 5.20–6.90, depending on the starting phosphate content. The presence of phosphate and carbonate ions favors the separation of Zn^{2+} as phosphate salt. By using biological HAP in massive form (cubelets measuring $\approx 3 \text{ mm}$) the reaction area is reduced and the adsorption of Zn^{2+} is limited, so if the Zn^{2+} -precipitating ions anions are failing with respect to the Zn^{2+} ion, this gives rise to an incomplete reaction. In all cases, the first crystalline phase formed is Hopeite and in our experimental conditions ($\text{pH} > 4$), there is no evidence of $ZnHPO_4 \cdot 3H_2O$.

Acknowledgment

We are grateful to University of Modena and Reggio Emilia for financial support.

References

1. R. Z. LEGEROS and J. P. LEGEROS, in "Phosphate Minerals", edited by J. O. Nriagu and P. B. Moore (Springer-Verlag, New York, 1984), p. 351.
2. L. J. SHYU, L. PEREZ, S. ZAWACKI, J. C. HEUGHEBAERT and G. H. NANCOLLAS, *J. Dental Res.* **62** (1983) 398.
3. J. LANG, *Bull. Soc. Sci. Brit.* **53** (1981) 95.
4. K. LADEFOGED, S. JARNUM, in "Zinc Deficiency Syndrome during Parenteral Nutrition in Humans, Metal Ions in Biological Systems", edited by H. Sigel, **15** (1983).
5. A. GERLACH, B. VINCENT, M. LISSAC, X. ESNOUF and G. THOLLET, *Biomaterials* **14** (1993) 770 and references therein.
6. R. E. GOING and J. C. MITCHEM *J. Am. Dent. Assoc.* **91** (1975) 107.
7. J. J. VIDEAU and V. DUPUIS, *Eur. J. Solid State Inorg. Chem.* **28** (1991) 303.
8. G. LUSVARDI, L. MENABUE and M. SALADINI, Proceedings 8th Cimtec Forum on New Materials, **35** (1994).
9. "Powder Diffraction File, Inorganic Phases", compiled by the Joint Committee of Powder Diffraction Standards, Swarthmore, PA (1989).
10. G. LUSVARDI, L. MENABUE, M. SALADINI and M. SPAGGIARI, *J. Mater. Chem.* **5** (1995) 493.
11. J. O. NRIAGU, in "Phosphate Minerals", edited by J. O. Nriagu and P. B. Moore (Springer-Verlag, New York, 1984), p. 325.
12. J. GAMBLE, in "Chemical Anatomy, Physiology and Pathology of Extracellular Fluid", 6th ed., (Harvard University, Cambridge, MA, 1967).
13. R. A. NYQUIST and R. O. KAGEL, in "Infrared Spectra of Inorganic Compounds ($3800\text{--}45 \text{ cm}^{-1}$)", (Academic Press, New York, 1973) p. 173.

Received 6 February 2000

and accepted 27 February 2001